Comparative Raman study of isostructural $YCrO_3$ and $YMnO_3$: Effects of structural distortions and twinning

N. D. Todorov,[1,*] M. V. Abrashev,[1] V. G. Ivanov,[1] G. G. Tsutsumanova,[1] V. Marinova,[2] Y.-Q. Wang,[3] and M. N. Iliev[3]

[1]*Faculty of Physics, University of Sofia, BG-1164 Sofia, Bulgaria*

[2]*Institute for Optical Materials and Technologies, Bulgarian Academy of Sciences, BG-1113 Sofia, Bulgaria*

[3]*Texas Center for Superconductivity and Department of Physics, University of Houston, Texas 77204-5002, USA*

(Received 30 March 2011; revised manuscript received 13 May 2011; published 21 June 2011)

Polarized Raman spectra of isostructural orthorhombic $YCrO_3$ and $YMnO_3$ single crystals were collected at the same conditions using different laser excitation in the visible range. The symmetry of the observed lines was determined and they were assigned to definite atomic vibrations based on lattice dynamical calculations. The frequencies of the lines of the same origin in both compounds are close, however, their intensities differ significantly. While the different intensity of the modes, activated by the Jahn-Teller distortion, can be explained by the different magnitude of this distortion in the two compounds, the cause of the reduced intensity of other lines in the low-frequency region in the Raman spectra of $YMnO_3$ is likely due to the fine twinning of the crystal.

DOI: 10.1103/PhysRevB.83.224303 PACS number(s): 78.30.Hv, 63.20.D−, 61.66.Fn

I. INTRODUCTION

The interest in the transition-metal perovskitelike oxides ABO_3 continues for decades because of many attractive phenomena observed in these compounds. Among them are structural second-order phase transitions, high-T_c superconductivity, colossal magnetoresistance, charge and orbital ordering, complex magnetic properties, etc. As a rule the structural, electrical, and magnetic properties of these compounds are strongly correlated. They can be tuned through the change of the mismatch of the A-O and B-O bond lengths, expressed by the tolerance factor $t = (R_A + R_O)/\sqrt{2}(R_B + R_O)$, where R_O, R_A, and R_B are the ionic radii of the oxygen and atoms in the A and B positions, respectively. Depending on the value of t, most of these compounds crystallize in superstructures of the ideal cubic perovskite (space group $Pm\bar{3}m$) with $R\bar{3}c$ or $Pnma$ symmetry. Using the model of Glazer,[1] treating the BO_6 octahedra as rigid ones, the superstructures can be obtained from the ideal cubic perovskite through some tilts (rotations) of the octahedra around the main crystallographic directions. In Glazer's notations, the rhombohedral $R\bar{3}c$ structure is of $(a^-a^-a^-)$ type and the orthorhombic $Pnma$ structure is of $(a^-b^+a^-)$ type.

Raman spectroscopy is a powerful experimental technique for study of perovskitelike oxides. Due to the fact that there are no Raman-active modes in the ideal cubic perovskite, all observed lines in the one-phonon region of the Raman spectra of the real perovskites have to be connected to some deviations of the real structure from the ideal one. For example, as shown in the pioneering work of Scott,[2] one of the Raman-active modes in the rare-earth aluminates of $R\bar{3}c$ structure consists in a rigid octahedral tilt around [111] direction. This mode can be considered as a "soft mode" and its frequency goes to zero as the temperature approaches the critical temperature of the structural second-order phase transition. Iliev *et al.*[3] have shown that in the case of rare-earth manganites with orthorhombic $Pnma$ structure, two of the observed lines in the Raman spectra originate from modes with a shape of the two static octahedral tilts existing in the structure. Although these compounds do not undergo second-order transition to a higher symmetry phase, the frequency of these lines directly scales the octahedral tilts as it is proportional to the tilt angle.

However, the model of rigid octahedra is inappropriate when the B ion is a Jahn-Teller (JT) ion (as the Mn^{3+}). In manganites the JT effect results in the presence of two pairs of Mn-O bonds of significantly different length and strongly deformed MnO_6 octahedra. For this reason, to explain the relationship between the intensity of the Raman lines and the structural distortions in orthorhombic manganites, a structural model accounting for four distortions (the two rotations from the Glazer model, the additional JT distortion, and the so-called A shift) was proposed.[4] Within the framework of the latter model, it can be concluded that the intensities of 20 out of the 24 Raman-active modes in the $GdFeO_3$-type structure are connected with only one of the above-mentioned distortions and the change of the intensities reflects the change of the structural distortions. Using this model it was possible to explain the significant difference of the relative intensity of the $B_{2g}(1)$ mode, activated by the JT distortion in the spectra of $CaMnO_3$ (containing the non-JT Mn^{4+} ion) and $YMnO_3$ (containing the JT Mn^{3+} ion). Unfortunately, the strong dependence of the intensity of many of the rest lines in the Raman spectra of $CaMnO_3$ on the excitation photon energy (i.e., the resonance effects) hampers the proof of the model in this case. In addition, the different charges of the A and B ions in $Y^{3+}Mn^{3+}O_3$ and $Ca^{2+}Mn^{4+}O_3$ impede the comparison of the Raman spectra of these two compounds.

For this reason we here present parallel Raman study of YBO_3 (B = Cr, Mn). The isostructural orthorhombic $Pnma$ compounds have close lattice parameters as well as close values of three of the four structural distortions, as defined in Ref. 4. The only difference is the presence of the JT distortion in $Mn^{3+}O_6$ octahedra, leading to their strong deformation, whereas the $Cr^{3+}O_6$ (Cr^{3+} is not a JT ion) octahedra are symmetric with nearly equal Cr-O bonds. The polarized Raman spectra of each compound, collected using laser excitation with different photon energy in the visible region, are practically identical, which shows that the resonance effects are negligible. It is worth noting here that this could not be concluded from the previous works[3,5–9] because

the spectra were obtained with a single laser line. Indeed, several papers on orthorhombic $YMnO_3$ report polarized[3,6,9] or nonpolarized[7,8] Raman spectra, obtained with either 515- or 633-nm laser excitation. For $YCrO_3$ there is only one early paper[5] on the polarized Raman spectra using 515 nm. In this work we show that there is a significant difference in the intensity of the $B_{2g}(1)$ line (activated by the JT distortion) in $YCrO_3$ and $YMnO_3$. Surprisingly, the intensity of other lines in the low-frequency region is strongly suppressed in $YMnO_3$, despite the close values of the activating structural distortions in both compounds. A comparison with the Raman spectra of other isostructural rare-earth perovskites leads to the conclusion that this is a result of a fine twinning of $YMnO_3$ single crystals.

II. EXPERIMENT

$YCrO_3$ single crystals were grown by a high-temperature solution growth method in Pt crucibles. We used Y_2O_3 and Cr_2O_3 as starting materials. A solid phase synthesis of stoichiometric powder $YCrO_3$ was performed at 1100 °C in an oxygen atmosphere for 48 h. We used complexes $PbF_2 : KF : B_2O_3$ in the ratio 0.75 : 0.23 : 0.02 as solvents. The ratio of the ground material $YCrO_3$ to the solvents was determined according to the phase diagrams[10,11] of the systems Y_2O_3, Cr_2O_3, and PbF_2. This ratio varies from 1/3 to 1/4. About 600 g of the mixture are semihermetically closed in the crucible with a cover in order to prevent the evaporation of PbF_2 and KF, which have a high vapor pressure at the growth process temperature. The temperature was increased at a rate of 50 °C/h to 1200 °C. To completely dissolve the components of the materials and to achieve a homogeneous solution, the temperature of 1200 °C was maintained for 48 h. Then the crucible was slowly cooled at a rate of 0.5 °C/h to 920 °C. At the final temperature the crucible was taken out of the oven, the cover was drilled through, and the solvent was poured out. The obtained crystals remained on the ground and the walls of the crucible.

Orthorhombic single crystals of $YMnO_3$ were synthesized by solid-state reaction under high pressure, described in Ref. 12. The chemical composition of the samples was confirmed using scanning electron microscope (SEM; Tescan LYRA) equipped with energy-dispersive x-ray spectrometer (EDX; Bruker). The SEM-EDX observations revealed that both types of crystals had a homogeneous composition of $Y : B = 1 : 1$ (B = Cr, Mn) without any impurities.

Polarized Raman spectra were obtained in backscattering geometry from several scattering configurations: xx, yy, zz, xz, and yx'. In this notation the first and the second letter shows the polarization of the incident and the scattered light, respectively, and x, y, z, and x' are parallel to the orthorhombic [100], [010], [001], and [101] crystal directions. It is not trivial to identify the orthorhombic ⟨100⟩ crystal directions. To do this we use the fact that all quasicubic perovskites have good cubic cleavage. This leads to almost perfect cubic shape of their microcrystals with the naturally grown surfaces of cubic {100} type; see Fig. 1. Additionally, preliminary measurements of polarized Raman spectra in special configurations according to these surface could be made. Only the orthorhombic [010] direction [$(010)_o$ surface] is perpendicular to the $\{010\}_c$ plane,

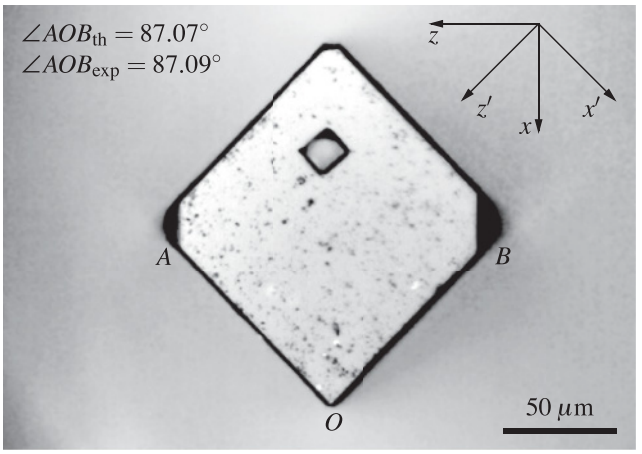

FIG. 1. Optical image of (010) surface of $YCrO_3$ single crystal. The notations used for the crystallographic directions are also given. Comparison of the calculated angle between the vertical (101) and $(\bar{1}01)$ orthorhombic surfaces (the crystal edges AO and BO in the photo) from the structural data[13] and measured angle directly from the image is done. The latter helps us to distinguish x and z directions.

so it can easily be identified. However, in $(010)_o$ surface the $[100]_o$ and $[001]_o$ directions are parallel to the diagonals (in the case of rhomblike surface) of the parallelogram-shaped surface. Because the lattice parameter $a_o > c_o$, it follows that the $[100]_o$ direction must be along the longer diagonal; see Fig. 1. The comparison of the angle between the $(101)_o$ and $(\bar{1}01)_o$ planes (that can be calculated from the published structural data[13]) with the measured angle between the crystal edges AO and BO in the photo in Fig. 1 is excellent.

The measurements were carried out using micro-Raman spectrometer LabRAM HR800 at room temperature. An objective ×100 was used both to focus the incident laser beam and to collect the scattered light. To check the presence of resonance effects in the Raman spectra, He-Ne (633 nm) and Ar^+ (514 and 458 nm) lasers were used as excitation sources. A small set of preliminary measurements, in which the product (laser power)×(acquisition time) remains constant, has been done to find out the appropriate power for which the overheating of the samples is negligible. Thus for both types of crystals and all laser lines the laser power used was about 2 mW. Due to the fine twinning of the $YMnO_3$ crystals, their nominally xx and zz spectra are identical. In contrast, the $YCrO_3$ crystals are twin free, as xx and zz spectra are significantly different (Fig. 2).

To facilitate the assignment of the Raman lines we performed shell-model lattice-dynamical calculations (LDC) based on interatomic potentials represented as a sum of long-range Coulomb potential and short-range potential in the Born-Mayer-Buckingham form $U_{\text{short-range}} = A\exp(-r/\rho) - C/r^6$. In this model an ion is divided into a core with charge Z, which represents the nucleus and the inner electrons of the ion and has all of its mass, and a massless shell with charge Y representing the valence electrons of the ion. The ionic polarizability α is accounted for as the interaction between the core and the shell. This interaction can be modeled with a harmonic spring of force constant k, then the polarizability is given by $\alpha = Y^2/k$. The calculations were carried out using

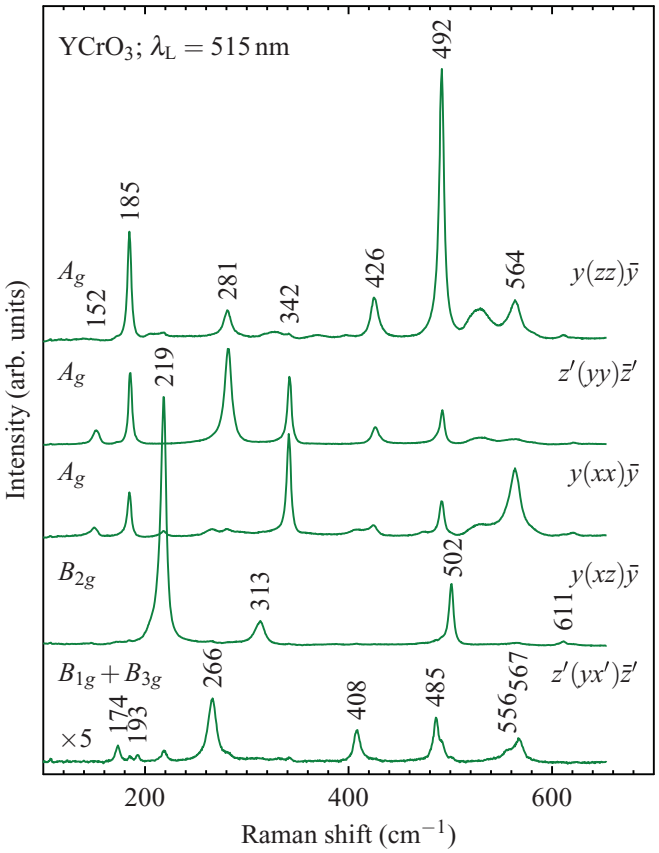

FIG. 2. (Color online) Polarized Raman spectra of $YCrO_3$ single crystal, obtained from (010) and (101) surfaces with 515-nm laser line. For better comparison, the $z'(yx')\bar{z}'$ spectrum is multiplied by 5, and the other spectra are shifted along the vertical axis for clarity.

the GULP code.[14] The parameters Z, Y, k, A, ρ, and C are listed in Table I. The cell parameters and atomic positions for $YMnO_3$ and $YCrO_3$, used in the calculations, are taken from Refs. 17 and 13.

III. DISCUSSION

The orthorhombic YBO_3 (B = Cr, Mn) crystals have $GdFeO_3$-type structure[13,17] (space group $Pnma$, $Z = 4$, $a_o \approx c_o \approx \sqrt{2}a_c$, $b_o \approx 2a_c$, where a_c is the lattice parameter of the ideal cubic perovskite). The group theory predicts $7A_g + 5B_{1g} + 7B_{2g} + 5B_{3g}$ Raman-active modes from the Γ point of the Brillouin zone.[18,19] The selection rules for these modes as well the symmetry-allowed directions of motion of the atoms, participating in them, are given in Refs. 4 and 6. Polarized Raman spectra, obtained from (010) and (101) surfaces of a $YCrO_3$ crystal with 515-nm laser excitation, are shown in Fig. 2. It is seen in spectra with xx, yy, and zz polarization that seven lines, observed at 152, 185, 281, 342, 426, 492, and 564 cm^{-1}, have A_g symmetry and they correspond to the predicted $7A_g$ modes. We observe an additional eight broad lines near 530 cm^{-1} also having A_g symmetry. The width of this line is more than two times larger than the width of the other A_g lines. Its irregular shape is not of Lorentz type and differs in xx, yy, and zz scattering configurations. Therefore we suppose that it does not originate from one-phonon Raman-allowed scattering, rather it has a two-phonon origin.

In the xz spectrum of $YCrO_3$ only four out of seven the Raman-allowed B_{2g} lines are observed. Comparison of yy and xz spectra of $YCrO_3$ and $YMnO_3$ (where all $7B_{2g}$ are seen), obtained with 633-, 515-, and 458-nm laser excitation, is made in Figs. 3 and 4, respectively. Their assignment to definite atomic vibrations, based on LDC, is also given. Due to the fact that all the faces of the naturally grown $YCrO_3$ crystals are with quasicubic {100} orientation, it was impossible to measure yx or yz spectra, where B_{1g} and B_{3g} lines could be observed separately. For this reason in Fig. 2 we present a spectrum with yx' polarization [obtained from the $(\bar{1}01)_o \equiv (100)_c$ surface], which contains both B_{1g} and B_{3g} lines. However, using the data presented by Udagawa *et al.*[5], as well as our LDC results, the symmetry of these lines also can be determined. In Table II are summarized the frequencies of the observed lines and the calculated ones by LDC in this paper as well previously published data (Ref. 5 for $YCrO_3$, Ref. 6 for $YMnO_3$). It is seen that the experimental results for $YMnO_3$ are practically identical.

In the previously published papers,[3,6,9] the Raman spectra of $YMnO_3$ were obtained only with 633-nm laser excitation. As it can be seen from Figs. 3 and 4, the relative intensity of the observed lines does not depend on the photon excitation energy. Comparing the results for $YCrO_3$ presented in Ref. 5 and here, because of the much better quality of our spectra, two more weak lines are detected (the line at 611 cm^{-1} of B_{2g} symmetry, and the line at 556 cm^{-1}, which, based on LDC, is a B_{1g} line). The lack of resonance effects holds also for the spectra of $YCrO_3$. On the other hand, from Figs. 3 and 4 it is seen that the relative intensity for lines, corresponding to one and the same mode in both compounds,

TABLE I. Parameters of the potentials of the shell-shell and core-shell interactions. Due to different values of k for the oxygen in $YMnO_3$ and $YCrO_3$ it is marked as O_{Mn} and O_{Cr}, respectively. All the potentials are taken from Ref. 15, except the one for Cr-O pair, which is from Ref. 16.

Ion	Z ($\|e\|$)	Y ($\|e\|$)	k ($e^2/Å^3$)	Ionic pair	A (eV)	ρ (Å)	C ($eV\,Å^6$)
Y	2.90			Y-O	1345.1	0.3491	0.000
Mn	0.30	2.80	51.20	Mn-O	715.8	0.3464	0.000
Cr	0.30	2.80	49.50	Cr-O	1763.0	0.2960	0.000
O_{Mn}	0.82	−2.82	53.72	O-O	22764.3	0.1490	27.879
O_{Cr}	0.82	−2.82	36.70	O-O	22764.3	0.1490	27.879

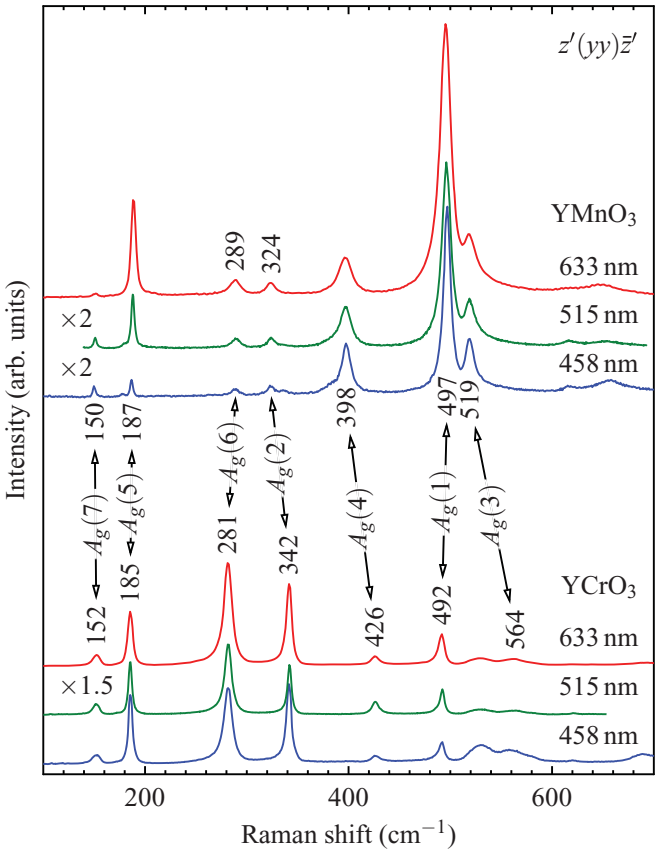

FIG. 3. (Color online) Raman spectra with $z'(yy)\bar{z}'$ polarization (where only A_g lines are allowed), obtained from (101) surfaces of $YMnO_3$ and $YCrO_3$ single crystals using different laser excitation. For better comparison some of the spectra are multiplied by a number, indicated in the figure. The assignment of the corresponding lines, based on the LDC, is also given.

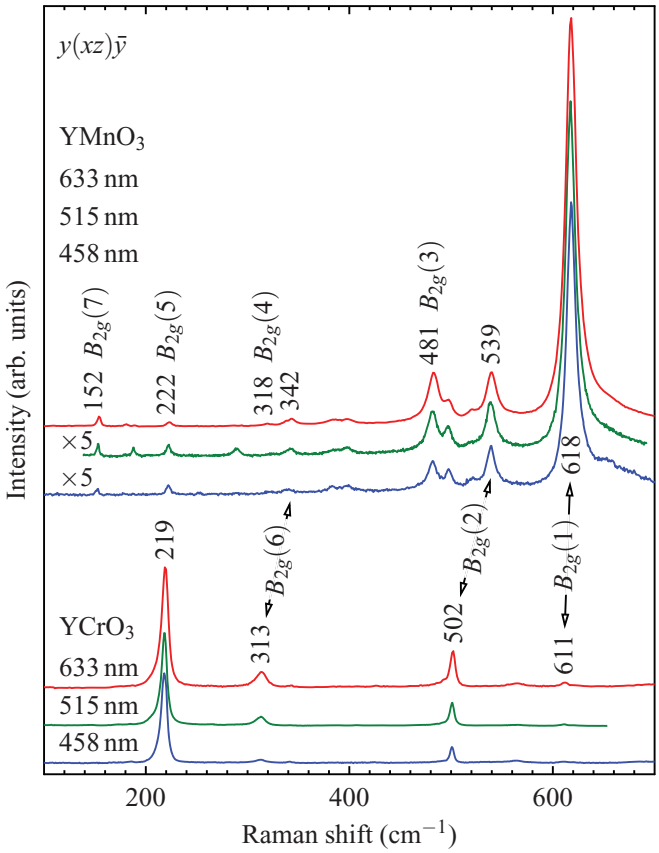

FIG. 4. (Color online) Raman spectra with $y(xz)\bar{y}$ polarization (where only B_{2g} lines are allowed), obtained from (101) surfaces of $YMnO_3$ and $YCrO_3$ single crystals using different laser excitation. For better comparison some of the spectra are multiplied by a number, indicated in the figure. The assignment of the corresponding lines, based on the LDC, is also given.

is very different. For example, the most intensive lines at 618 (B_{2g}) and 497 cm^{-1} (A_g) in the $YMnO_3$ are very weak in $YCrO_3$, where they correspond to the lines at 611 and 492 cm^{-1}. In contrast, the most intensive lines in $YCrO_3$ [219 cm^{-1} (B_{2g}) and 281 and 342 cm^{-1} (A_g)] are very weak in $YMnO_3$. In general, the intensity of a line in a Raman spectrum in a specific geometrical configuration is a complex function of the electronic structure of the compound, the energy of the incident photons, the specifics of the crystal structure, and the geometrical configuration. However, in our case of YBO_3 (B = Cr, Mn) there is no dependence of the relative intensity of a line on the exciting photon energy. Therefore it is plausible to assume that this intensity is determined mainly by the structural distortion. In the model, proposed in Ref. 4, and adapted for this type of structure, it is concluded that the intensity of the most (20 out of 24) Raman-active lines is governed mainly by only one structural distortion and it will monotonously increase with its value. The assignment of the Raman-active modes and the structural distortion activating them are shown in Table II (the numbering of the modes follows the notations from Ref. 4).

In Table III are given the values, calculated from structural data, of the four structural distortions for some perovskites. The values of rotational distortions $D_{[101]}$ and $D_{[010]}$ (in degrees) are calculated according to the formulas $D_{[101]} = \arctan(2\,|x_{O2} - z_{O2}|)$ and $D_{[010]} = \arctan(\frac{2\sqrt{2}|z_{O1}|+4\sqrt{2}|y_{O2}|}{2})$, where x_{O2}, z_{O2}, z_{O1}, and y_{O2} are the deviations of the fractional coordinates of oxygen atoms O1 and O2 from their positions in the idealized structure without this type of distortion.[4] As seen from Table III, the values of $D_{[101]}$, $D_{[010]}$, and DA-shift distortions in $YMnO_3$ and $YCrO_3$ are close, whereas the value of D_{JT} is by a factor of 6 larger in $YMnO_3$ compared to $YCrO_3$. Only the $B_{2g}(1)$ mode (in-phase stretching vibration of O2 atoms) is activated solely by D_{JT}. Indeed, the line corresponding to this mode in $YMnO_3$ is the most intensive one, while in $YCrO_3$ it is very weak. Moreover, the second in intensity $A_g(1)$ line in $YMnO_3$ is also activated by D_{JT}. On the other hand, in the Raman spectra of ABO_3 perovskites, containing non-JT ion in the B position (or an JT ion, which does not produce a large difference in the B-O2 distances, as is the case of Ti^{3+}), the $B_{2g}(1)$ line is either weak or even not detectable [see, e.g., B = Al,[25] Sc,[26,27] Ti,[28,29] V,[30] Fe,[31,32] Ni (Ref. 33)]. Therefore it appears that the intensity of the $B_{2g}(1)$ line can be used as a measure of the JT distortion of the BO_6 octahedra.

The intensity of other A_g and B_{2g} lines in the low-frequency range (below 350 cm^{-1}) in the spectra of $YCrO_3$ is rather strong compared to the corresponding lines in the spectra of

TABLE II. Comparison between experimental (from this paper and previously published results) and calculated frequencies of the Raman-active lines in $YCrO_3$ and $YMnO_3$. The symmetry of the lines, the assignment (based on LDC) to the definite atomic vibrations, and the activating distortions (according to Ref. 4) are also given.

	$YCrO_3$			$YMnO_3$				
Symmetry	Ref. 5	Expt.	Calc.	Ref. 6	Expt.	Calc.	Assignment	Activating distortion
A_g	156	152	152	151	150	165	7	*A*shift
A_g	188	185	185	188	187	217	5	[010]
A_g	282	281	229	288	289	265	6	*A* shift
A_g	346	342	298	323	324	302	2	[010], JT
A_g	429	426	384	396	398	373	4	[101]
A_g	492	492	429	497	497	483	1	[010], JT
A_g	566	564	493	518	519	498	3	[101]
B_{2g}			160	151	152	179	7	*A* shift
B_{2g}	223	219	209	220	222	234	5	[101]
B_{2g}			274	317	318	297	4	[101]
B_{2g}	318	313	339	341	342	351	6	*A* shift
B_{2g}			444	481	481	497	3	[101]
B_{2g}	502	502	461	537	539	523	2	[010]
B_{2g}		611	611	616	618	618	1	JT
B_{1g}			193	205	205	226	5	*A* shift
B_{1g}	272	266	267	284	285	269	4	[010], JT
B_{1g}	413	408	329	383	382	327	3	[101]
B_{1g}		556	466			414	2	[101]
B_{1g}			611			647	1	*A* shift
B_{3g}	176	174	152	178	179	184	5	[101]
B_{3g}			308	336	337	332	4	[010], JT
B_{3g}	487	485	440			410	3	[101]
B_{3g}	569	567	482			491	2	[101]
B_{3g}			619			642	1	[101]

$YMnO_3$ [except for the $A_g(5)$ line, which has comparable intensity in both compounds]. This is somewhat puzzling as both compounds have comparable values of the three other structural distortions, responsible for the intensity. Moreover, the comparison of the polarized Raman spectra (in particular those with *yy* polarization) of other isostructural compounds shows that all seven A_g lines have a relative intensity[27,30] similar to that of $YCrO_3$. The reasonable question is why is the intensity of these lines in $YMnO_3$ is so different? It seems that the reason is not in the large value of the JT distortion but rather in the twinning. It can be found that practically all synthesized and investigated single crystals from the type $A^{3+}B^{3+}O_3$ (A^{3+}: rare-earth ion), except the manganites, are not twinned, whereas all single crystals of manganites are twinned in the (010) plane (the same plane where the JT orbital ordering holds). Actually, there is only one report[34] on untwinned $LaMnO_3$ single crystal. In this case the untwinned crystal has been found by chance among the majority of twinned crystals in the ingot and probably it has been naturally detwinned by appropriately oriented uniaxial stress in a small region in the crucible during the cooling. Due to the fact that the size of the twin domains is much smaller than 1 μm (the diameter of the laser beam used), a considerable part of atoms in the structure are close to a twin boundary and therefore they have an incoherent and variable atomic environment, leading to depression of the corresponding Raman lines. This hypothesis can be proved in a parallel Raman study of twinned and detwinned manganite crystals.

TABLE III. The values of the structural distortions of several YBO_3 compounds (B = Al, Ti, V, Cr, Mn) and $NdBO_3$ (B = Sc, Ni).

Compound	$D_{[101]}$ (deg)	$D_{[010]}$ (deg)	D_{JT}	DA-shift	Ref.
$YAlO_3$	13.7	10.3	0.0000	0.1062	20
$NdScO_3$	17.5	12.1	0.0054	0.1064	21
$YTiO_3$	18.5	13.4	0.0020	0.1458	22
YVO_3	17.6	12.8	0.0102	0.1388	23
$YCrO_3$	16.7	12.2	0.0084	0.1324	13
$YMnO_3$	16.8	14.2	0.0542	0.1710	17
$NdNiO_3$	11.8	8.0	0.0070	0.0700	24

IV. CONCLUSIONS

Single crystals of $YCrO_3$ and finely twinned crystals of $YMnO_3$ were studied by micro-Raman spectroscopy in backscattering geometry at room temperature with different scattering configurations. The symmetry of the observed lines was determined from the polarized spectra. In comparison to a previous paper[5] for $YCrO_3$ two new lines, B_{1g} and B_{2g} at 556 and 611 cm^{-1}, are registered. Based on performed lattice dynamical calculations the observed lines are assigned to definite atomic vibrations. The lines in the spectra of $YCrO_3$ and $YMnO_3$, corresponding to the same modes, have close frequencies, but significantly different relative intensities. The

large intensity of two of the lines [$B_{2g}(1)$ and $A_g(1)$] in $YMnO_3$ is explained by the presence of a large Jahn-Teller distortion. The low intensity of the rest lines in the spectra of $YMnO_3$, if compared to these in $YCrO_3$, cannot be explained accounting for the structural distortions. It is concluded that the reduced intensity of these lines is caused by the fine twinning of the manganite crystals related to the JT ordering.

ACKNOWLEDGMENTS

This work was supported in part by Grants No. DO02-167/2008, No. DO02-56/2008, and No. TK-X-1712/2007 of the Bulgarian National Science Fund, Grant No. 25/2011 of the Science Fund of the University of Sofia, as well as by the State of Texas through the Texas Center for Superconductivity at the University of Houston (TcSUH).

*neno@phys.uni-sofia.bg

[1] A. M. Glazer, Acta Crystallogr., Sect. B **28**, 3384 (1972).
[2] J. F. Scott, Phys. Rev. **183**, 823 (1969).
[3] M. N. Iliev, M. V. Abrashev, J. Laverdière, S. Jandl, M. M. Gospodinov, Y.-Q. Wang, and Y.-Y. Sun, Phys. Rev. B **73**, 064302 (2006).
[4] M. V. Abrashev, J. Bäckström, L. Börjesson, V. N. Popov, R. A. Chakalov, N. Kolev, R.-L. Meng, and M. N. Iliev, Phys. Rev. B **65**, 184301 (2002).
[5] M. Udagawa, K. Kohn, N. Koshizuka, T. Tsushima, and K. Tsushima, Solid State Commun. **16**, 779 (1975).
[6] M. N. Iliev, M. V. Abrashev, H.-G. Lee, V. N. Popov, Y. Y. Sun, C. Thomsen, R. L. Meng, and C. W. Chu, Phys. Rev. B **57**, 2872 (1998).
[7] I. Martín-Carrón, A. de Andrés, M. J. Martínez-Lope, M. T. Casais, and J. A. Alonso, J. Alloys Compd. **323-324**, 494 (2001).
[8] L. Martín-Carrón and A. de Andrés, J. Alloys Compd. **323-324**, 417 (2001).
[9] J. Laverdière, S. Jandl, A. A. Mukhin, V. Y. Ivanov, V. G. Ivanov, and M. N. Iliev, Phys. Rev. B **73**, 214301 (2006).
[10] W. Wong-Ng, R. S. Roth, T. A. Vanderah, and H. F. McMurdie, J. Res. Natl. Inst. Stand. Technol. **106**, 1097 (2001).
[11] M. Yoshimura, M. Jayaratna, and S. Somiya, J. Am. Ceram. Soc. **65**, c166 (1982).
[12] M. N. Iliev, B. Lorenz, A. P. Litvinchuk, Y.-Q. Wang, Y. Y. Sun, and C. W. Chu, J. Phys.: Condens. Matter **17**, 3333 (2005).
[13] K. Ramesha, A. Llobet, T. Proffen, C. R. Serrao, and C. N. R. Rao, J. Phys.: Condens. Matter **19**, 102202 (2007).
[14] J. D. Gale, J. Chem. Soc., Faraday Trans. **93**, 629 (1997).
[15] G. V. Lewis and C. R. A. Catlow, J. Phys. C **18**, 1149 (1985).
[16] M. N. Iliev, A. P. Litvinchuk, V. G. Hadjiev, Y.-Q. Wang, J. Cmaidalka, R.-L. Meng, Y.-Y. Sun, N. Kolev, and M. V. Abrashev, Phys. Rev. B **74**, 214301 (2006).
[17] J. A. Alonso, M. J. Martínez-Lope, M. T. Casais, and M. T. Fernández-Diáz, Inorg. Chem. **39**, 917 (2000).
[18] M. I. Aroyo, A. Kirov, C. Capillas, J. M. Perez-Mato, and H. Wondratschek, Acta Crystallogr., Sect. A **62**, 115 (2006).
[19] M. I. Aroyo, J. M. Perez-Mato, C. Capillas, E. Kroumova, S. Ivantchev, G. Madariaga, A. Kirov, and H. Wondratschek, Z. Kristallogr. **221**, 15 (2006).
[20] N. Ross, J. Zhao, and R. Angel, J. Solid State Chem. **177**, 1276 (2004).
[21] B. Veličkov, V. Kahlenberg, R. Bertram, and M. Bernhagen, Z. Kristallogr. **222**, 466 (2007).
[22] M. Cwik, T. Lorenz, J. Baier, R. Müller, G. André, F. Bourée, F. Lichtenberg, A. Freimuth, R. Schmitz, E. Müller-Hartmann, and M. Braden, Phys. Rev. B **68**, 060401 (2003).
[23] G. R. Blake, T. T. M. Palstra, Y. Ren, A. A. Nugroho, and A. A. Menovsky, Phys. Rev. B **65**, 174112 (2002).
[24] J. L. García-Muñoz, M. A. G. Aranda, J. A. Alonso, and M. J. Martínez-Lope, Phys. Rev. B **79**, 134432 (2009).
[25] A. Casu, P. C. Ricci, and A. Anedda, J. Raman Spectrosc. **40**, 1224 (2009).
[26] C. Girardot, J. Kreisel, S. Pignard, N. Caillault, and F. Weiss, Phys. Rev. B **78**, 104101 (2008).
[27] O. Chaix-Pluchery and J. Kreisel, Phase Transit. **84**, 542 (2011).
[28] M. Reedyk, D. A. Crandles, M. Cardona, J. D. Garrett, and J. E. Greedan, Phys. Rev. B **55**, 1442 (1997).
[29] M. N. Iliev, A. P. Litvinchuk, M. V. Abrashev, V. N. Popov, J. Cmaidalka, B. Lorenz, and R. L. Meng, Phys. Rev. B **69**, 172301 (2004).
[30] S. Miyasaka, J. Fujioka, M. Iwama, Y. Okimoto, and Y. Tokura, Phys. Rev. B **73**, 224436 (2006).
[31] N. Koshizuka and S. Ushioda, Phys. Rev. B **22**, 5394 (1980).
[32] S. Venugopalan, M. Dutta, A. K. Ramdas, and J. P. Remeika, Phys. Rev. B **31**, 1490 (1985).
[33] M. Zaghrioui, A. Bulou, P. Lacorre, and P. Laffez, Phys. Rev. B **64**, 081102 (2001).
[34] V. Skumryev, F. Ott, J. Coey, A. Anane, J.-P. Renard, L. Pinsard-Gaudart, and A. Revcolevschi, Eur. Phys. J. B **11**, 401 (1999).